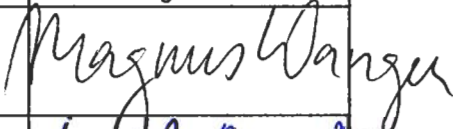
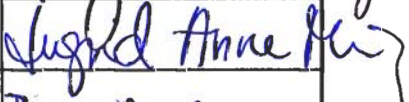



KJELLER		HALDEN	
Address	NO-2027 Kjeller, Norway	NO-1751 Halden, Norway	
Telephone	+47 63 80 60 00	+47 69 21 22 00	
Telefax	+47 63 81 55 53	+47 69 21 22 01	
Report number		Date	
IFE/KR/E-2005/004		2005-06-02	
Report title and subtitle		Number of pages	
Sandstone porosity related to vitrinite reflectance		32	
Project/Contract no. and name		ISSN	
		0333-2039	
Client/Sponsor Organisation and reference		ISBN	
		82-7017-519-6	
Abstract			
<p>The volume fraction of quartz cement is a measure of a sandstones thermal exposure, and vitrinite reflectance (VR) is another measure of the thermal exposure. It is shown how the porosity reduction from quartz cementation can be related to VR for heating at a constant rate by using simple models for quartz cementation and VR. This relationship shows that the heating rate appears as an explicit parameter, which means that there is no pure relationship between porosity (volume fraction quartz cement) and VR. However, it turns out that the rate of quartz cementation and the rate of change of TTI have exponential dependence of temperature that is close. Porosity reduction by quartz cementation as a function of VR is therefore nearly the same curve for very different temperature histories. This property of porosity reduction by quartz cementation is utilized to calibrate the parameters in the average specific surface as function of the porosity. The calibration procedure is demonstrated on two data sets, and the average specific surface depends on the porosity to the power of an exponent that is a little larger than 3 for these data sets.</p>			
Keywords: vitrinite reflectance, quartz cementation, mapping of kinetics			
	Name	Date	Signature
Author(s)	Magnus Wangen	2005-06-02	
Reviewed by	Ingrid Anne Munz	2005-06-02	
Approved by	Björg Andresen	2005-06-02	

1 Introduction

Vitrinite reflectance (VR) is a widely used thermal indicator in sedimentary basin that is routinely measured in most exploration wells. The VR values can be grouped into immature, oil generative, gas generative and exhausted, and they are therefore used as a direct measurement of the degree of maturity of the rock.

VR is an expression of the impact of a temperature-history on the rock. Quartz cementation is also a process that depends on the temperature history, (Walderhaug 1994a, 1994b, Oelkers *et al.* 1996, 2000, Bjørkum 1994, 1996). One would therefore expect a relationship between the progress of quartz cementation and VR, because both are functions of the time-temperature history. A connection between porosity and VR has been studied in a series of papers by Schmoker and co-workers, (Schmoker and Gautier 1988, 1989, Schmoker and Higley 1991, Schmoker and Schenk 1994, Kopaska-Merkel and Schmoker 1994) and Hayes (1991). Schmoker and co-workers have correlated $\log_{10} \phi$, (where ϕ is the porosity), with $\log_{10}(\text{TTI})$ and $\log_{10}(\%Ro)$, where TTI is the time-temperature-integral of Lopatin and %Ro is the vitrinite reflectance. This paper follows the idea of expressing the porosity as a function of TTI and %Ro. It is in particular the porosity of sandstones that can be expressed as a function of TTI and %Ro using simple models for quartz cementation.

Expressing sandstone porosity as a function of TTI and %Ro is an example of the general problem of expressing the progress (ϕ) of one kind of process with the progress (%Ro) of another process, where both processes are based on Arrhenius kinetics. A modeling approach to the mapping of one kind of time-temperature impact to another shows when we can expect such relations to exist, and what such a relationship might be. The use of VR as a measure of the maturity stages of hydrocarbon generation is an analogous application. Both VR and hydrocarbon generation are processes modeled with Arrhenius kinetics, and where the progress of VR is used as a measure of the progress of hydrocarbon generation.

It is important to point out that it is only the porosity reduction caused by quartz cementation that is expressed as a function of VR. The mechanical compaction of sand is controlled by the effective vertical stress, and is not a function of the temperature-history, (Chuan *et al.* 2002). However, mechanical compaction becomes arrested when the sandstone is buried to a sufficient depth for quartz cementation to start, (Bjørkum *et al.* 1998, Bjørkum and Nadeau 1998).

The paper is organized as follows: A short review of models for VR and the model for quartz cementation are first presented. Then follows how the porosity can be expressed as a function of TTI and %Ro for constant heating rates. Examples

with piecewise linear temperature histories are given, and it is shown how the parameters in the specific surface area can be calibrated with a set of porosity and VR observations. Two data sets are studied with the proposed model, before a conclusion is given.

2 Time-temperature-integral and VR

There are various models that allow VR to be calculated from a given temperature history, (Waples 1980, Larter 1989). The simplest approach is based on the time-temperature integral (TTI) of Lopatin, (Lopatin 1971), as done by for instance Waples (1980). Later models introduced by Burnham and Sweeny (1989), Larter (1989) and Sweeny and Burnham (1990) are based on Arrhenius kinetics. These models use multi-step Arrhenius kinetics to compute a transformation ratio, which is converted to VR by use of an exponential function.

We will begin with TTI based VR because it allows for simple expressions of the sandstone porosity as a function of the TTI and %Ro, when quartz cementation controls the porosity reduction. The TTI for a given temperature history is

$$\text{TTI} = \int_{t_0}^{t_1} b_I e^{a_I T(t)} dt \quad (1)$$

where $T(t)$ is the temperature in °C, and where t is the time in units s, (see table 1). The parameter a_I tells how TTI is related exponentially to the temperature, and the parameter b_I is a scaling factor, (Lopatin 1971). The TTI integral is an expression of the observation made by Lopatin that the rate of hydrocarbon generation doubles for every temperature step of 10 °C. The integral (1) for TTI is rewritten using the base of the natural logarithm, which turns out to be convenient in the following. The TTI can be computed exactly for a constant heating rate c (°C Ma⁻¹),

$$\text{TTI} = \frac{b_I}{a_I c} \left(e^{a_I T_2} - e^{a_I T_1} \right) \quad (2)$$

where T_1 and T_2 are the temperatures at the beginning and the end of the time interval of heating, respectively, and where the heating rate is $c = (T_2 - T_1)/(t_2 - t_1)$. The temperature at the start of the heating becomes less important when the temperature at the end of the heating interval is sufficiently high, $\exp(a_I(T_2 - T_1)) \gg 1$, because TTI can then be approximated as

$$\text{TTI} \approx \frac{b_I}{a_I c} e^{a_I T_2} \quad (3)$$

The time-temperature integral is converted to VR by the exponentiation

$$\%Ro = \exp(p \ln(TTI) + q) \quad (4)$$

where p and q are parameters. It is seen that %Ro is proportional to TTI to the power of the parameter p with e^q as a scaling factor. There is no unique set of p and q values, but several sets of parameters have been calibrated for different wells and burial histories, (Morrow and Issler 1993).

3 Quartz cementation using Walderhaug's precipitation rate

Several different models have been suggested for the often large volume fractions of quartz cement found in many deeply buried sandstones. An often used explanation is fluid flow, where quartz is believed to have precipitated from supersaturated fluids flowing through the sandstones. It has been pointed out that a very large volume of supersaturated fluid is needed to import all the observed silica, and fluid flow is therefore not likely to be a general explanation, (Bjørlykke 1993, Bjørlykke, *et al.* 1988). It has been argued that thermal convection cells could be a possible cause for the high fluid fluxes needed, where dissolution takes place at one end of the circular current and where precipitation takes place at the other end, (Wood and Hewett 1984). On the other hand, it turns out that the permeability, the layer thickness and thermal gradient needed for onset of thermal convection is rarely met, (Bjørlykke *et al.* 1988, Wangen 1994).

A more likely explanation is an internal source for the silica. A commonly used explanation is dissolution of quartz at grain contacts by pressure-solution. Pressure solution leads to dissolution of quartz in the fluid film at the quartz grain contacts, because the solubility of quartz is increasing with increasing pressure. The dissolved silica at the grain contacts is transported by diffusion in the fluid film towards the pore, where it precipitates as quartz cement, (Weyl 1955, Rutter 1983, De Boer 1977, Tada and Siever 1989, Dysthe *et al.* 2002). Although a physically viable explanation petrographic studies of quartz cemented sandstone do not support the idea of pressure solution at quartz-quartz contacts, (Oelkers *et al.* 1996). It is observed by cathodeluminescence that the detrital quartz grains remain intact under the quartz overgrowth. The source for silica found as cement in the sandstones has instead been related to dissolution along stylolites or other quartz-mica contacts, which are common features in most sandstones, (Heald 1959, Oelkers *et al.* 1996). How mica enhances dissolution is studied both experimentally and

theoretically, but it is not fully understood, (Weyl 1959, Tada and Siever 1989). The silica dissolved at the stylolites is transported by diffusion into the pore space in between the stylolites where it precipitates as cement, (Aase *et al.* 1996, Oelkers *et al.* 1996, Walderhaug 1996). Petrographic studies show that precipitation is the slowest step in the overall process of dissolution at the stylolites, transport of silica by diffusion, and precipitation in the pore space. The silica supersaturation between the stylolites is therefore almost constant, (Oelkers *et al.* 1996, 2000).

It has been possible to estimate the quartz cementation rates as a function of temperature, (Walderhaug 1994a, 1994b). Walderhaug found that the rate of quartz cementation as a function of temperature can be expressed as

$$r(T) = b_\phi e^{a_\phi T}, \quad (5)$$

in units $\text{mole m}^{-2}\text{s}^{-1}$, where $b_\phi = 1.98 \cdot 10^{-18} \text{ mole m}^{-2}\text{s}^{-1}$ and $a_\phi = 0.051 \text{ 1/}^\circ\text{C}$, (see table 1). Walderhaug's expression for the rate of quartz precipitation can be turned into an expression for the rate of change of porosity,

$$\frac{d\phi}{dt} = -v_q S(\phi) r(T) \quad (6)$$

where v_q ($\text{m}^3\text{mole}^{-1}$) is the molar volume of quartz and where $S(\phi)$ (m^2/m^3) is the specific surface of the pore space as a function of the porosity. (The specific surface is the effective surface area of the pore space divided by the volume of the sample.) The specific surface will decrease as the pore space is filled with cement. A function that tells how the specific surface depends on the porosity is required in order to predict the porosity. A simple choice for specific surface as a function of the porosity is

$$S(\phi) = S_0 \hat{S}_n(\phi) \quad \text{and} \quad \hat{S}_n(\phi) = \left(\frac{\phi - \phi_c}{\phi_0 - \phi_c} \right)^n \quad (7)$$

where S_0 is the specific surface at the onset of cementation. The function $\hat{S}_n(\phi)$ is equal to one for $\phi = \phi_0$, the porosity at the onset of cementation, and zero for ϕ_c . The porosity ϕ_c is the minimum porosity where the pore space becomes disconnected. The exponent n controls how the specific surface decreases towards zero with decreasing porosity. The specific surface function (7) is assumed to represent pore space of a sandstone at a macroscopic scale, and it is therefore the average specific surface for a sandstone. For this reason it may be different from exact models of the specific surface for a homogeneous pore space with a constant grain size. For example a straightforward scaling argument used by Lichtner (1988) gives an exponent $n = 2/3$. The porosity modelling that has been carried out by Bjørkum (1996), Oelkers *et al.* (1996, 2000) and Walderhaug (1996)

is based on a linear function (7), ($n = 1$). Figure 1 shows the dimensionless specific surface \hat{S} for $n = 1/2, 1, 2, 3$ and 4. There exist analytical relationships between the specific surface and the porosity for different types of random homogeneous porous media (Weissberg 1963) and random heterogeneous porous media (Torquato 1991), and equation (7) can be considered a simple mean to approximate both exact and empirical relationships. The Fountainebleu sandstones is an example of a sandstone where the specific surface area have been studied in the laboratory during dissolution and fluid flow, (Kieffer *et al.* 1999, Jove *et al.* 2003).

Equation (6) can be integrated to an expression for the porosity as a function of time or temperature when it is assumed that heating takes place at a constant rate c ($^{\circ}\text{C Ma}^{-1}$), (Walderhaug 1996, Wangen 1999, 2000). (See the appendix for details.)

4 Porosity as a function of TTI for constant heating rates

Both TTI and the porosity during quartz cementation is given as exponential functions of the temperature. There are unfortunately no general and simple way to express the temperature dependence of porosity with the temperature dependence of TTI, except when both $\exp(a_{\phi}(T_2 - T_1)) \gg 1$, $\exp(a_I(T_2 - T_1)) \gg 1$, and when the heating rate is constant. (A generalization to piecewise linear temperature histories follows later.) Given these assumptions there is an expression for the porosity as a function of TTI, as shown by equations (25) and (26) in the appendix. It is seen from these equations that most parameters from both quartz cementation and TTI are coming together in the (dimensionless) number N_{ϕ} , (see the appendix). The exceptions are the initial porosity, minimum porosity and the exponent in the specific surface function. An important observation is that the heating rate is also present in the number N_{ϕ} . Ideally, we would like every aspect of the temperature history to be represented only by TTI in the expressions (25) and (26) for the porosity. The fact that the heating rate c turns up as an explicit parameter in addition to TTI shows that TTI alone cannot be used to represent the temperature history for quartz cementation. The relationship (27) shows that the only exception is when $a_{\phi} = a_I$, i.e. when both processes have the same exponential rate dependence of temperature. The standard parameter values for a_{ϕ} and a_I shows that $a_{\phi}/a_I \approx 0.73$, (see table 1), which is close to 1, and the dependence on the heating rate therefore turns out to be weak.

It is convenient to plot the sandstone porosity as a function of $\ln(\text{TTI})$, because TTI grows to the power of T . It follows from expression (25) that

$$\ln(-\ln \hat{\phi}) \approx \frac{a_\phi}{a_I} \ln(\text{TTI}) + \ln(N_\phi) \quad (8)$$

where $\hat{\phi}$ is the normalized porosity $(\phi - \phi_c)/(\phi_0 - \phi_c)$. The normalized porosity $\hat{\phi}$ is 1 at the onset of cementation and decreases towards 0 with increasing cementation. The porosity has to be represented as $f_1 = \ln(-\ln \hat{\phi})$, for $n = 1$, in order to become a straight line when plotted as a function of $\ln(\text{TTI})$. A specific surface exponent different from 1 implies that the porosity has to be represented by

$$f_n = \ln \left(\frac{\hat{\phi}^{1-n} - 1}{(n-1)} \right) \quad (9)$$

(The representation f_n approaches f_1 when $n \rightarrow 1$.) It is also seen that a constant specific surface (independent of porosity) is given by $n = 0$, and that $f_0 = \ln(1 - \hat{\phi})$ is linearly related to $\ln(\text{TTI})$. These particular representations of the porosity (f_0 , f_1 and f_n) are directly related to expression (7) for the specific surface as a function of the porosity. A different relationship for the specific surface than expression (7) implies another representation of the porosity in order to have a linear relationship in $\ln(\text{TTI})$. The expression for f in the case of a general function $\hat{S}(\hat{\phi})$ for the specific surface as a function of the porosity is

$$f(\hat{\phi}) = \ln \left(\int_{\hat{\phi}}^1 \frac{d\hat{\phi}}{\hat{S}(\hat{\phi})} \right) \quad (10)$$

as shown in the appendix. (Equation (10) yields expressions f_0 , f_1 and f_n .) This is a hint about the importance the specific surface plays in porosity reduction by quartz cementation. It is therefore the integral of the inverse specific surface that becomes a straight line of $\ln(\text{TTI})$. Under reasonable assumptions there will always be a one-to-one relationship between f and ϕ , so ϕ can be mapped to f and visa versa.

The straight line plotted as function of $\ln(\text{TTI})$ has the steepness given by the ratio a_ϕ/a_I , which is the temperature exponent for quartz cementation relative to the exponent of TTI. The number N_ϕ gives the porosity in terms of a f -value for $\text{TTI} = 1$, where for example $\hat{\phi} = e^{-N_\phi}$ for $n = 1$.

The porosity reduction by quartz cementation during constant heating is not only a function of TTI, but also an explicit function of the heating rate. The dependence on the heating rate is in the term $\ln(N_\phi)$. That implies that the porosity development for different heating rates becomes lines with the same steepness, but with

different offset. The (dimensionless) number N_ϕ can be rewritten as

$$N_\phi = \left(\frac{c}{c_p} \right)^{(a_\phi/a_I)-1} \quad (11)$$

in terms of the ratio of the heating rate and a reference heating rate. The reference heating rate c_p is defined by the relations (27) and (11). The porosity represented as f_n can then be plotted as

$$f_n \approx \frac{a_\phi}{a_I} \ln(\text{TTI}) + \left(\frac{a_\phi}{a_I} - 1 \right) \ln\left(\frac{c}{c_p} \right) \quad (12)$$

which shows the heating rate dependence explicitly. The factor $1 - (a_\phi/a_I) = 0.27$, which means that the dependence on the heating rate is weak, (since the absolute value of the factor is close to zero). The straight lines for two heating rates, where one is a factor 2 higher than the other, are separated vertically by $0.27 \ln(2) \approx 0.19$.

5 Porosity as a function of %Ro for constant heating rates

Similar expressions to those for the porosity as a function of TTI and $\ln(\text{TTI})$ can be made using %Ro, because of the linear relationship (4) between the $\ln(\text{TTI})$ and $\ln(\%Ro)$, (see equations (28) and (29) in the appendix). These expressions can be written as

$$f_n \approx \left(\frac{a_\phi}{a_I p} \right) \ln(\%Ro) + \ln(N_R) \quad (13)$$

in terms of $\ln(\%Ro)$, (see appendix). All three expressions (28), (29) and (13) are derived under the assumption of heating at a constant rate. It is the porosity represented by f_n , or the integral (10) in case of general specific surface function, that becomes a straight line when plotted as a function of $\ln(\%Ro)$. Although the preceding derivations are carried out with empirical rate laws for quartz cementation and %Ro, it is reasonable to expect that these rate laws show real trends when they are combined.

The straight line relationship (13) has two parameters, similar to f_n as a function of $\ln(\text{TTI})$, which are the steepness $a_\phi/(a_I p)$ and the offset $\ln(N_R)$. It is seen that the steepness of the line is $a_\phi/(a_I p) \approx 4$, with the parameter values from table 1. The number N_R depends on the heating rate in a similar way to the number N_ϕ ,

which can be shown explicitly as

$$f_n = \left(\frac{a_\phi}{a_I p} \right) \ln(\%Ro) + \left(\frac{a_\phi}{a_I} - 1 \right) \ln\left(\frac{c}{c_R} \right), \quad (14)$$

where

$$N_R = \left(\frac{c}{c_R} \right)^{(a_\phi/a_I)-1} \quad (15)$$

and where the reference heating rate c_R is defined in terms of N_R using equation (30). The factor $1 - (a_\phi/a_I) = 0.27$ is close to 0 and the dependence on the heating rate is therefore weak.

Another way to write the porosity representation f_n is to emphasize the initial specific surface S_0 by writing

$$f_n \approx \left(\frac{a_\phi}{a_I p} \right) \ln(\%Ro) + \ln\left(\frac{S_0}{S_R} \right) \quad (16)$$

where the reference specific surface S_R is defined by $N_R = S_0/S_R$. This may be a convenient way to write the porosity (or f_n) as a function of $\ln(\%Ro)$ when the initial specific surface S_0 and the specific surface exponent n that are free tuning parameters.

The porosity as a function of temperature for different constant heating rates are plotted in figure 2a. The parameters used in figure 2a are given by table 1, except for the heating rates. Heating is from 0 °C to 180 °C for the four time intervals 260 Ma, 130 Ma, 65 Ma and 32.5 Ma. It is seen from figure 2a that slow heating to 180 °C lead to earlier porosity reduction than rapid heating. The same porosity history is also plotted as a function VR in figure 2b. Slow heating rates leads to larger VR values at the end temperature 180 °C. When the latter plot is converted to a plot of f as a function $\ln(\%Ro)$ then the curves become straight lines, as shown in figure 2c. The vertical offset between the lines is $(1 - (a_\phi/a_I))\ln(2) = 0.2$, because the different lines represent a doubling of the heating rate.

6 Piecewise linear temperature histories

The temperature history of a sandstone is rarely caused by heating at a constant rate. A data set with porosity as a function VR from the same formation will contain samples with different temperature histories. A large scatter in the VR-values indicates that the temperature history has been different for the different

samples. It turns out that the porosity plotted as f -values of $\ln(\%Ro)$ follows approximately the same line for different temperature histories given that all other parameters are the same. Figure 2c shows that f -values of $\ln(\%Ro)$ for four different heating rates are given by four closely spaced lines. The influence of the temperature history is studied further in figures 3a to 3d. Figure 3a shows the f -values as a function of $\ln(\%Ro)$ for the different temperature histories shown in figure 3b. Figure 3c shows the porosity as a function of $\%Ro$ and figure 3d shows the porosity as a function of time. Figures 3a and 3c show that the porosity follow roughly the same curve when plotted as a function of $\%Ro$ even for temperature histories that are quite different. It is therefore possible to use heating at a constant rate to reproduce a given linear relationship between f -values and $\ln(\%Ro)$ -values.

7 Calibration of the specific surface area

An observed linear relationship between f -values and $\ln(\%Ro)$ -values can be reproduced using heating at a constant rate, which means that a detailed knowledge of the temperature history is not needed. This allows the average specific surface of a formation to be estimated without the use of a detailed temperature history. The parameters S_0 and n in the specific surface function (7) are the only (free) tuning parameters apart from a heating rate. The other parameters involved, like the parameters for TTI, $\%Ro$ and quartz cementation, are given. It is the average specific surface that is obtained by matching the line (13) against a data set, because different samples will most likely have a specific surface that is different from the average of the full data set. The optimal values for the initial specific surface S_0 and the exponent n are therefore the parameters that best describes the average specific surface for the entire sandstone formation.

A data set of porosity and VR measurements has to be converted into a corresponding set of f_n and $\ln(\%Ro)$ -values in order to be analyzed with relationship (13). The f_n -values should then be distributed along a straight line when plotted as a function of $\ln(\%Ro)$. The optimal straight line $A \ln(\%Ro) + B$ that fits a data set is found using least square minimization. The numbers A and B from least square minimization must match the line (13). The steepness A of this line should be equal to the steepness $a_\phi / (a_{Ip})$ of the line (13). The only way to match the A -parameter is to tune the specific surface exponent n that controls the f_n values. In other words, the exponent n has to be tuned so that A from least square minimization of the data becomes the same as the (fixed) steepness required by the line (13).

Once the optimal exponent n is found, and the data fit a line with the given steepness, it is the offset B that has to match $\ln(N_R)$ of the line (13). The expression for the line (13) is based on heating at a constant rate. It is therefore no unique value for S_0 that makes $\ln(N_R) = B$, because there is no unique choice for a heating rate. From the equality $\ln(N_R) = B$ it follows that

$$S_0 = \exp\left(B + \frac{qa_\phi}{pa_I}\right) \left(\frac{(\phi_0 - \phi_c)a_\phi}{v_q b_\phi}\right) \left(\frac{b_I}{a_I}\right)^{(a_\phi/a_I)} c^{(a_\phi/a_I)-1} \quad (17)$$

where S_0 depends on the heating rate to the power of $(a_\phi/a_I) - 1 = -0.27$. The initial specific surface S_0 is therefore increasing by one order of magnitude when the heating rate is reduced by a factor 5000. A reasonable guess for a heating rate may therefore be used to obtain an order of magnitude estimate for the optimal (average) initial specific surface.

8 Results

The calibration of the specific surface as a function of the porosity is demonstrated on two data sets. The first data set is given by Schmoker and Higley (1991) for the Lower Cretaceous J sandstone in the Denver basin of Colorado, and it covers 31 widely separated wells. The VR values from the same well are not expected to vary much because the formation thickness does not exceed 46 m, and it is generally less than 30 m. Several core-plug porosity measurements were carried out for each well, (with an average of 31 measurements per well), and the porosity measurements are reported as histograms that show the 10th, 25th, 50th, 75th and 90th percentile, (Schmoker and Higley, 1991). The geological setting, petrography and the full data sets are found in Schmoker and Higley (1991), where they correlate the porosity to VR with equation $\phi = a(\%Ro)^b$ using least square regression. The data used here is taken from table 3 in Schmoker and Higley (1991), where the 50th percentile of the porosity is related to the VR-measurements. The J sandstone is treated as a single unit as was done by Schmoker and Higley (1991). The 50th percentile of the porosity represented as f -values is plotted as a function of $\ln(\%Ro)$ in figure 4. The optimal value of the exponent in the specific surface function is $n = 3.15$ as seen from figure 5. Figure 5 shows the steepness A of the linear least square minimization as a function of the exponent n . The horizontal line in figure 5 is the steepness required by the line of equation (13). The offset from linear least square minimization B was matched using the initial specific surface of equation (17), with a constant heating rate $10 \text{ }^\circ\text{C/Ma}$. The initial specific surface is then $S_0 = 2.5 \cdot 10^5 \text{ m}^2/\text{m}^3$. The porosity at the onset of the cementation

was set to $\phi_0 = 0.26$ and the minimum porosity was set to $\phi_c = 0.03$. There is a trend in the data set although the J sandstone is not an ideal quartzose sandstone.

A similar calibration of the specific surface was carried out for the Upper Jurassic Norphlet Formation in southwestern Alabama, using data reported in a study of porosity correlated to VR by Schmoker and Schenk (1994). The geological setting, petrography, review of data preparation and an extensive reference to the work done on the Norphlet formation is given in Schmoker and Schenk (1994). The calibration of specific surface using the data in table 1 and 2 of in Schmoker and Schenk (1994) is shown in figure 6. The data is plotted as f_n -values of $\ln(\%Ro)$ for $n = 3.5$. The optimal exponent n is shown in figure 5, where the steepness A of the linear least square minimization is plotted for the n in the interval 0 to 6. The offset B from linear least square minimization was matched using the initial specific surface from equation (17) with a constant heating rate $c = 10$ °C/Ma. The initial specific surface corresponding to B then becomes $S_0 = 1.1 \cdot 10^4$ m²/m³. The initial specific surface for the Norphlet sandstone is almost an order of magnitude less than the initial specific surface of the J sandstone, which is consistent with the observations of Schmoker and Schenk (1994) that the Norphlet sandstone has a high average porosity compared with sandstone formations in other basins with the same maturity.

These two sandstones are different with respect to the porosity, which is reflected by the initial specific surface. However, the exponent n , which tells how the specific surface decrease with decreasing porosity, are comparable for the two different sandstones, (3.15 for the J sandstone and 3.5 for the Norphlet sandstone). An exponent larger as large as 3 is different from what could be expected from simple models of porous media, which predict an exponent close to 1, (Torquato 1991). The reason for this difference is likely to be the heterogeneous nature of sandstones. A large exponent n also reflects the fact that the porosity approaches the minimum porosity in a smooth manner with increasing temperature during burial, (Wangen 1999, 2000). An exponent n less than one implies that the minimum porosity will be reached at finite temperature, (Wangen 1999, 2000). But larger data sets and several more calibrations have to be carried out in order to establish that an exponent n as large as 3 is a common behavior for the specific surface of sandstones.

9 Conclusion

The porosity reduction caused by quartz cementation is related to the thermal exposure of the rock expressed as VR. A simple relationship is derived between

the porosity and VR for heating at a constant rate. The expression for porosity as a function of VR is based on Walderhaug's (Walderhaug 1994a, 1994b) empirical expression for the rate of quartz cementation, and VR related to TTI. It is used that the rate of change of TTI has the same form as the empirical rate law for quartz cementation. The expression for the porosity as a function of VR for heating at a constant rate shows that the heating rate appears explicitly. It is therefore not possible to use quartz cementation as an equivalent measure of the thermal exposure as VR, because the conversion of VR to volume fraction quartz cement involves the heating rate, or in general the temperature history. However, the dependence on the heating rate turns out to be weak, because the exponents in the empirical rate law for quartz cementation and TTI are close. It is shown with numerical examples that the porosity as a function of VR follows nearly the same curve for very different temperature histories.

It is possible to represent the porosity by the inverse specific surface integrated over the porosity. This representation of the porosity becomes a straight line when plotted as a function of $\ln(\%Ro)$ for heating at a constant rate. It is shown that different temperature histories yield nearly the same line as the one that results from heating at a constant rate. This linear relationship between the representation of the porosity and $\ln(\%Ro)$ allows the function for the average specific surface to be calibrated with a data set. The average specific surface function is taken to be a proportional to an initial value for onset of cementation and to the porosity to the power of a given exponent. It is shown how these two parameters in the function for the average specific surface can be optimized using a data set of measured porosity and VR values. Two examples are given based on the data sets of Schmoker and Higley (1991) and Schmoker and Schenk (1994), respectively. The data sets have exponents in the specific surface function that are 3.15 and 3.5, respectively. It might therefore be that the average specific surface does not depend linearly on the porosity, but on the porosity to power of an exponent that is close to 3.

Although the suggested relationship between porosity and VR is based on simple models for quartz cementation and VR, it may serve as a useful method to calibrate the average specific surface of a sandstone formation.

10 Appendix

Equation (6) for the rate of change of porosity can be written as

$$\frac{d\hat{\phi}}{\hat{S}(\hat{\phi})} = -\frac{v_q S_0 b_\phi}{\phi_0 - \phi_c} e^{a_\phi T(t)} dt. \quad (18)$$

This equation can be integrated as follows

$$\int_1^{\hat{\phi}} \frac{d\hat{\phi}}{\hat{S}(\hat{\phi})} = -\frac{v_q S_0 b_\phi}{(\phi_0 - \phi_c) a_\phi c} (e^{a_\phi T_2} - e^{a_\phi T_1}) \quad (19)$$

for heating from the temperature T_1 to T_2 in the time interval from t_1 to t_2 with the constant heating rate $c = (T_2 - T_1)/(t_2 - t_1)$. The porosity is ϕ_0 at the beginning of the heating, which corresponds to $\hat{\phi} = 1$. The right-hand-side of equation (19) can be integrated in the case of the specific surface function (7), and the porosity becomes

$$\phi = \phi_c + (\phi_0 - \phi_c) \exp\left(-N_b (e^{a_\phi T_2} - e^{a_\phi T_1})\right) \quad (20)$$

for the specific surface exponent $n = 1$, and

$$\phi = \phi_c + (\phi_0 - \phi_c) \left(1 - (1 - n) N_b (e^{a_\phi T_2} - e^{a_\phi T_1})\right)^{1/(1-n)} \quad (21)$$

for the specific surface exponent $n \neq 1$, where the number N_b is

$$N_b = \frac{S_0 v_q b_\phi}{(\phi_0 - \phi_c) a_\phi c} \quad (22)$$

We notice that most parameters involved in porosity reduction appear only once, and that is as a factor in the number N_b .

Assuming that $\exp(a_\phi T_2) \gg \exp(a_\phi T_1)$ and that TTI can be approximated by equation (3) we get that

$$\int_1^{\hat{\phi}} \frac{d\hat{\phi}}{\hat{S}(\hat{\phi})} \approx -N_\phi \text{TTI}^{(a_\phi/a_I)} \quad (23)$$

This equation can be written as

$$f = \frac{a_\phi}{a_I} \ln(\text{TTI}) + \ln(N_\phi) \quad (24)$$

where f is defined by equation (9). When the specific surface is given by equation (7), we get the following relationship between the porosity and the TTI,

$$\phi \approx \phi_c + (\phi_0 - \phi_c) \exp\left(-N_\phi \text{TTI}^{(a_\phi/a_I)}\right) \quad (25)$$

for specific surface exponent $n = 1$, and

$$\phi \approx \phi_c + (\phi_0 - \phi_c) \left(1 - (1 - n)N_\phi \text{TTI}^{(a_\phi/a_I)}\right)^{1/(1-n)} \quad (26)$$

for specific surface exponent $n \neq 1$, where

$$N_\phi = N_b \left(\frac{a_{IC}}{b_I}\right)^{(a_\phi/a_I)} \quad (27)$$

The porosity can be related %Ro by use of the relationship (4) between %Ro and TTI, which gives that

$$\phi \approx \phi_c + (\phi_0 - \phi_c) \exp\left(-N_R \%Ro^{(a_\phi/a_I p)}\right) \quad (28)$$

for specific surface exponent $n = 1$, and

$$\phi \approx \phi_c + (\phi_0 - \phi_c) \left(1 - (1 - n)N_R \%Ro^{(a_\phi/a_I)}\right)^{1/(1-n)} \quad (29)$$

for specific surface exponent $n \neq 1$, where

$$N_R = \exp\left(-\frac{qa_\phi}{pa_I}\right)N_\phi \quad (30)$$

The (dimensionless) number N_R includes the parameters for quartz cementation, TTI and %Ro.

11 References

- Aase, N.E, Bjørkum, P.A. and Nadeau, P.H., 1996, The effect of grain coating micro-quartz on preservation of reservoir porosity, *AAPG Bulletin*, **80**, no. 10, p. 1654-1673.
- Bjørkum, P.A., 1994, How important is pressure in causing dissolution of quartz in sandstones?, (abs.): AAPG Annual Meeting Program with Abstracts, **3**, p. 105.
- Bjørkum, P.A., 1996, How important is pressure in causing dissolution of quartz in sandstones?, *Journal of Sedimentary Research*, **66**, no. 1, p. 147-154.
- Bjørkum, P.A., Oelkers, E.H., Nadeau, P.H., Walderhaug, O. and Murhpy, W.M., 1998, Porosity prediction in quartzose sandstones as a function of time, temperature, depth, stylolite frequency, and hydrocarbon saturation, *AAPG Bulletin*, **82**, no. 4, p. 637-648.
- Bjørkum, P.A. and Nadeau, P.H., 1998, Temperature controlled porosity/permeability reduction, fluid migration, and petroleum exploration in sedimentary basins, *Australian Petroleum Production and Exploration Association Journal*, **38**, part 1, p. 453-464.
- Bjørlykke, K., Mo, A. and Palm, E., 1988, Modelling of thermal convection in sedimentary basins and its relevance to diagenetic reactions, *Marine and Petroleum Geology*, **5**, p. 338-351.
- Bjørlykke, K., 1993, Fluid flow in sedimentary basins, *Sedimentary Geology*, **86**, p. 137-138.
- Burnham, A.K., Sweeney, J.J., 1989, A chemical kinetic model of vitrinite maturation and reflectance, *Geochimica et Cosmochimica Acta*, **53**, no 10, p. 2649-2657.
- Chuan, F.A., Kjeldstad, A., Bjørlykke, K. and Høeg, K., 2002, Porosity loss in sand by grain crushing - experimental evidence and relevance to reservoir quality, *Marine and Petroleum Geology*, **19**, p. 39-53.
- De Boer, R.B., 1977, On the thermodynamics of pressure solution - interaction between chemical and mechanical forces, *Geochimica et Cosmochimica Acta*, **41**, p. 249-256.
- Dysthe, D.K., Podladchikov, Y., Renard, F., Feder, J. and Jamtveit, B., 2002, Universal scaling in transient creep, *Physics Review Letters*, **89** (24) art. no. 246102.
- Hayes, J.B., 1991, Porosity evolution of sandstones related to vitrinite reflectance,

- Organic Geochemistry*, **17**, no. 2, p. 117-129.
- Heald, M.T., 1955, Stylolites in sandstones, *Journal of Geology*, **63**, p. 101-114.
- Jove, C.F., Oelkers, E.H., and Schott, J., 2003, An experimental study of porosity, reactive surface area and permeability evolution during dissolution of the Fontainebleau sandstone, *Geochimica et Cosmochimica Acta*, **68**, p. 805-817.
- Kieffer, B., Jove, C.F., Oelkers, E.H., and Schott, J., 1999, An experimental study of the reactive surface area of the Fontainebleau sandstone as a function of porosity, permeability and fluid flow rate, *Geochimica et Cosmochimica Acta*, **63**, p. 3525-3534.
- Kopaska-Merkel, D.C. and Schmoker, J.W., 1994, Regional porosity evolution in the Smackover formation of Alabama, *Carbonates and Evaporites*, **9**, no. 1, p. 58-75.
- Larter, S., 1989, Chemical models of vitrinite reflectance evolution, *Geologische Rundschau*, **78** (1), p. 349-359.
- Lichtner, P.C., 1988, The quasi stationary state approximation to coupled mass transport and fluid-rock interaction in a porous medium, *Geochimica et Cosmochimica Acta*, **52**, p. 143-165.
- Lopatin, N.V., 1971, Temperature and geological time as a factor in coalification, *Izv. Akad. Nauk. SSSR, Ser. Geol.*, **3**, p. 95-106.
- McKenzie, D.P., 1981, The variation of temperature with time and hydrocarbon maturation in sedimentary basins formed by extension, *Earth and Planetary Science Letters*, **55**, p. 87-98.
- Morrow, D.W. and Issler, D.R., 1993, Calculation of vitrinite reflectance from thermal histories: Comparison of some methods, *AAPG Bulletin*, **77**, no. 4, p. 610-624.
- Oelkers, E.H., Bjørkum, P.A. and Murphy, W.M., 1996, A petrographic and computational investigation of quartz cementation and porosity reduction in North Sea sandstones, *American Journal of Science*, **296**, p. 420-452.
- Oelkers, E.H., Bjørkum, P.A., Walderhaug, O., Nadeau, P.H. and Murphy, W.M., 2000, Making diagenesis obey thermodynamics and kinetics: the case of quartz cementation in sandstones from offshore mid-Norway, *Applied Geochemistry*, **15**, p. 295-309.
- Rutter, E.H., 1983, Pressure solution in nature, theory and experiments, *Journal*

of Geological Society London, **140**, p. 725-740.

Schmoker, J.W. and Gautier, L.G., 1988, Sandstone porosity as a function of thermal maturity, *Geology*, **16**, p. 1007-1010.

Schmoker, J.W. and Gautier, D.L., 1989, Compaction of basin sediments: Modeling based on time-temperature history, *Journal of Geophysical Research*, **94**, no. B6, p. 7379-7386.

Schmoker, J.W. and Higley, D.K., 1991, Porosity trends of the Lower Cretaceous J Sandstone, Denver basin Colorado, *Journal of Sediment Petrology*, **61**, no. 6, p. 909-920.

Schmoker, J.W. and Schenk, C.J., 1994, Regional porosity trends of the Upper Jurassic Norphlet formation in Southwestern Alabama and Vicinity, with comparisons to Formations of other basins, *AAPG Bulletin*, **78**, no. 2, p. 166-180.

Sweeney, J.J. and Burnham, A.K., 1990, Evaluation of a simple model of vitrinite reflectance based on chemical kinetics, *Am. Assoc. Pet. Geol., Bull.*, **74**, p. 1559-1570.

Tada, R. and Siever, R., 1989, Pressure solution during diagenesis, *Annual Review of Earth Planetary Science*, **17**, p. 89-118.

Torquato, S., 1991, Random heterogeneous media: Microstructure and improved bounds on effective properties, *Applied Mechanics Reviews*, **44**, no. 2, p. 37-76.

Walderhaug, O., 1994a, Temperatures of quartz cementation in Jurassic sandstones from the Norwegian continental shelf- evidence from fluid inclusions, *Journal of Sedimentary Research*, **A64**, no. 2, p. 311-323.

Walderhaug, O., 1994b, Precipitation rates for quartz cement in sandstones determined by fluid-inclusion microthermometry and temperature history modeling, *Journal of Sedimentary Research*, **A64**, no. 2, p. 324-333.

Walderhaug, O., 1996, Kinetic modeling of quartz cementation and porosity loss in deeply buried sandstone reservoirs, *AAPG Bulletin*, **80**, no. 5, p. 731-745.

Wangen, M., 1994, Numerical simulation of thermal convection in compacting sedimentary basins, *Geophysical Journal International*, **119**, p. 129-150.

Wangen, M., 1999, Modeling quartz cementation of quartzose sandstones, *Basin Research*, **11**, p. 113-126.

Wangen, M., 2000, Generation of overpressure by cementation of pore space in sedimentary rocks, *Geophysical Journal International*, **143**, p. 608-620.

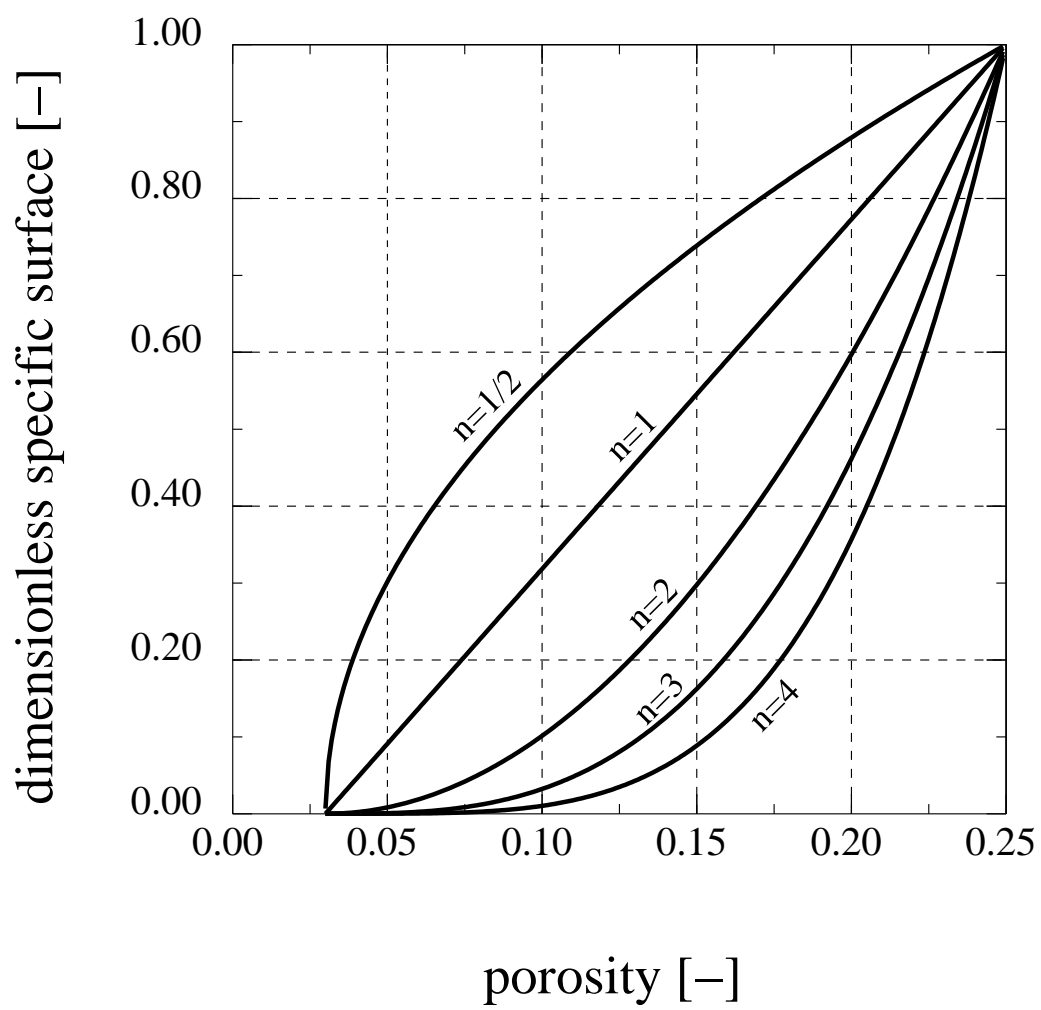
Waples, D.W., 1980, Time and temperature in petroleum formation: application of Lopatins method to petroleum exploration, *Am. Assoc. Pet. Geol., Bull.*, **64**, p. 916-926.

Weissberg, H.J., 1963, Effective diffusion coefficient in porous media, *Journal of Applied Physics*, **34**, no. 9, p. 2636-2639.

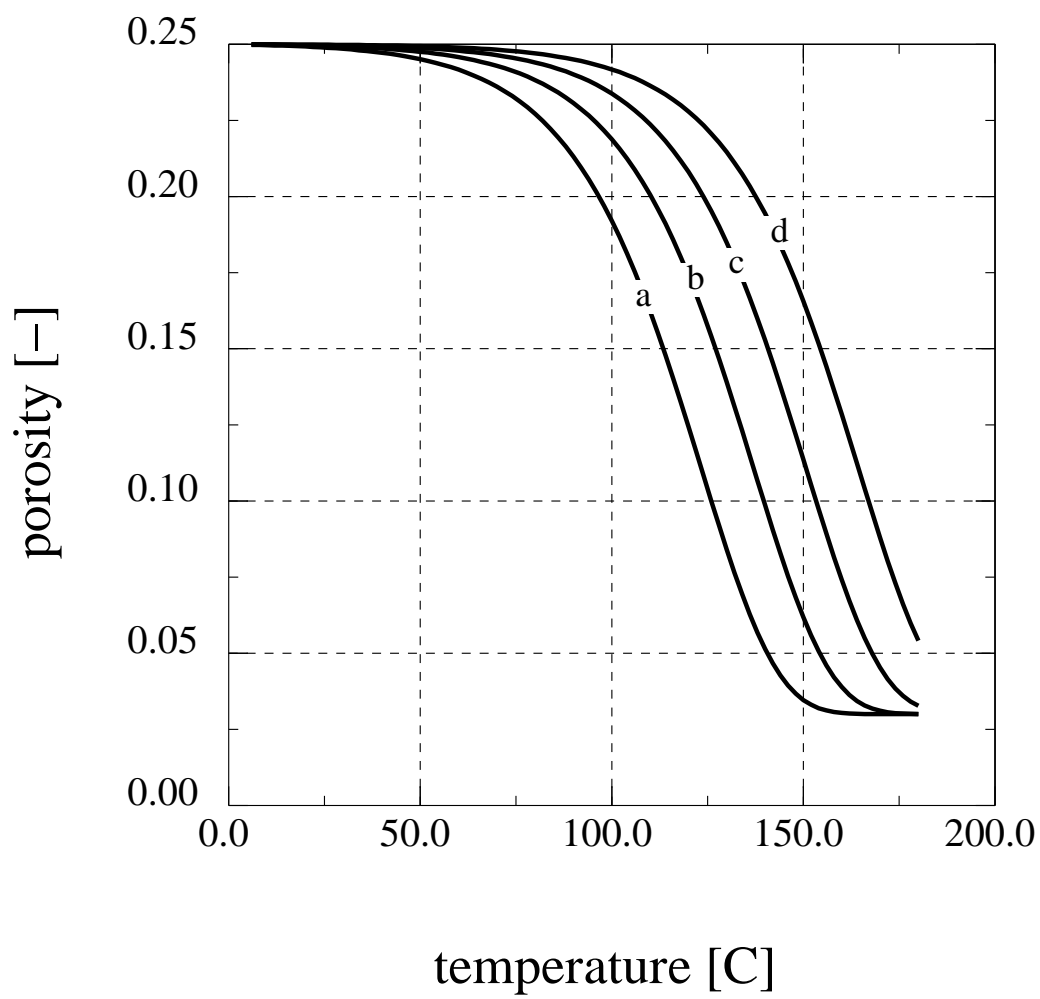
Weyl, P.K., 1959, Pressure solution and the force of crystallization - a phenomenological theory, *Journal of Geophysical Research*, **64**, p. 2001-2025.

WOOD, J.R., AND HEWETT, T.A., 1984, Reservoir diagenesis and convective fluid flow, in D.A. McDonald and R.C. Surdam, des., *Clastic diagenesis: AAPG Memoir 37*, p. 99-110.

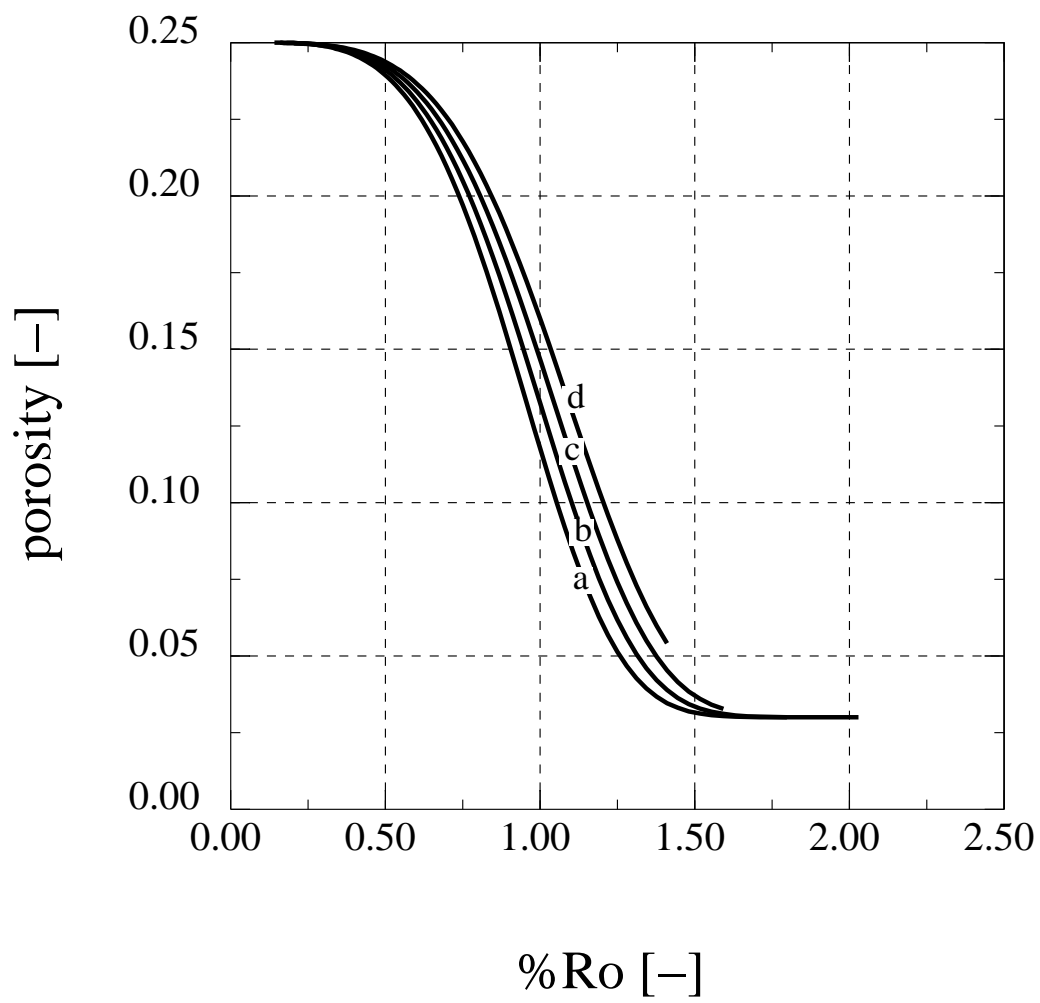
12 Figures



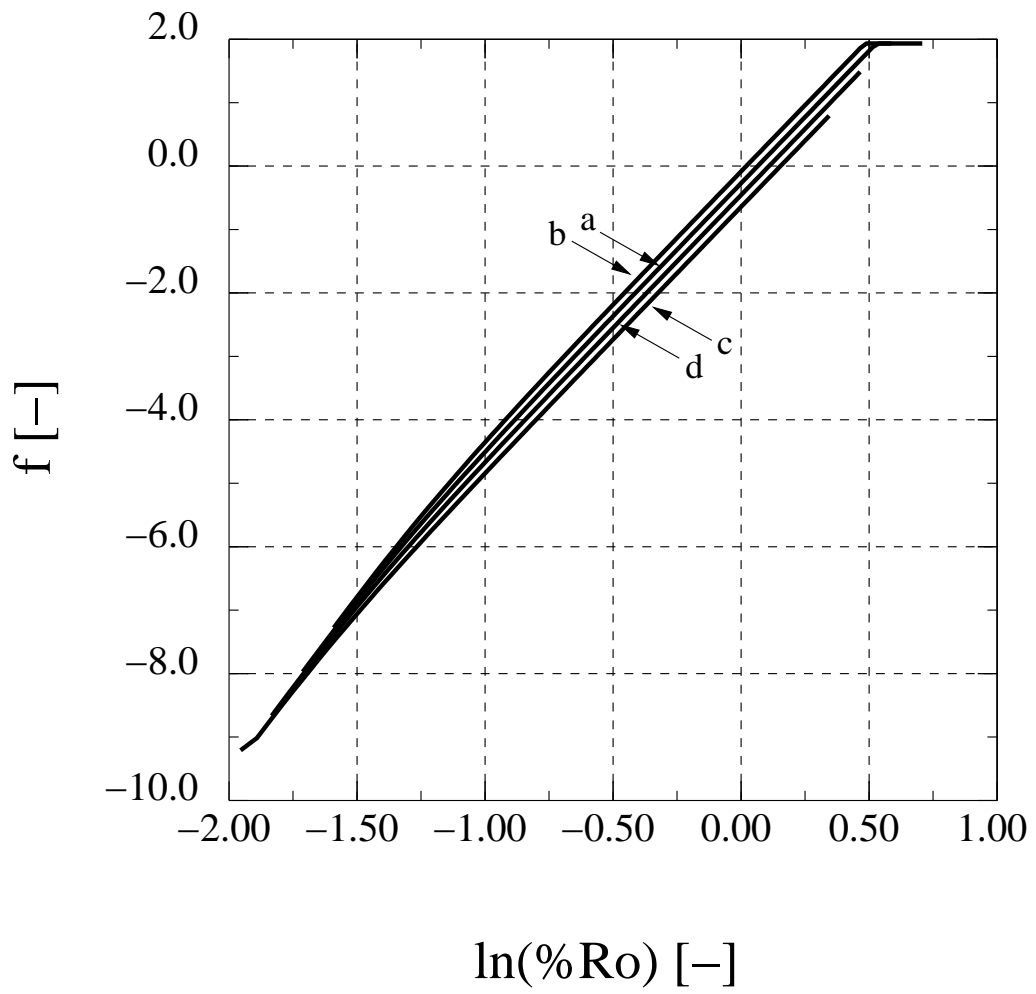
file: fig1.eps



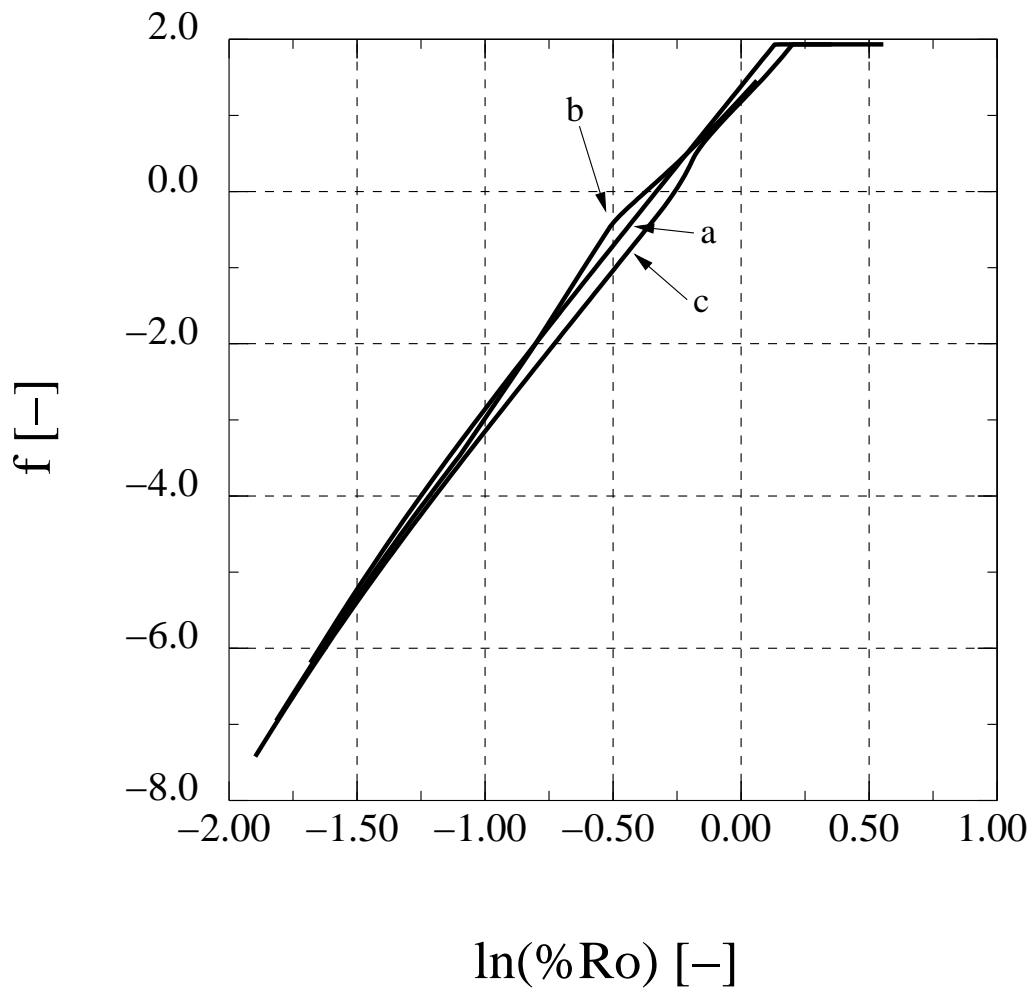
file: fig2a.eps



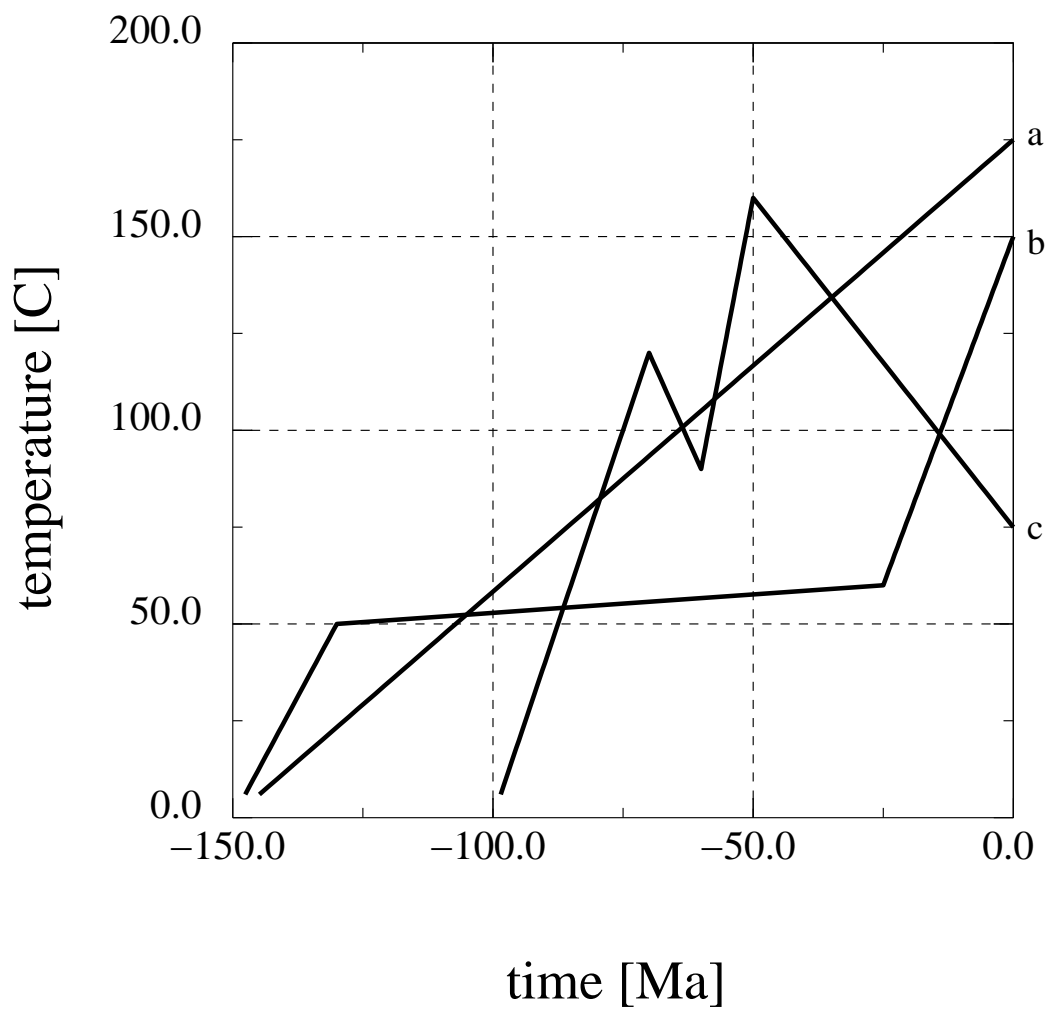
file: fig2b.eps



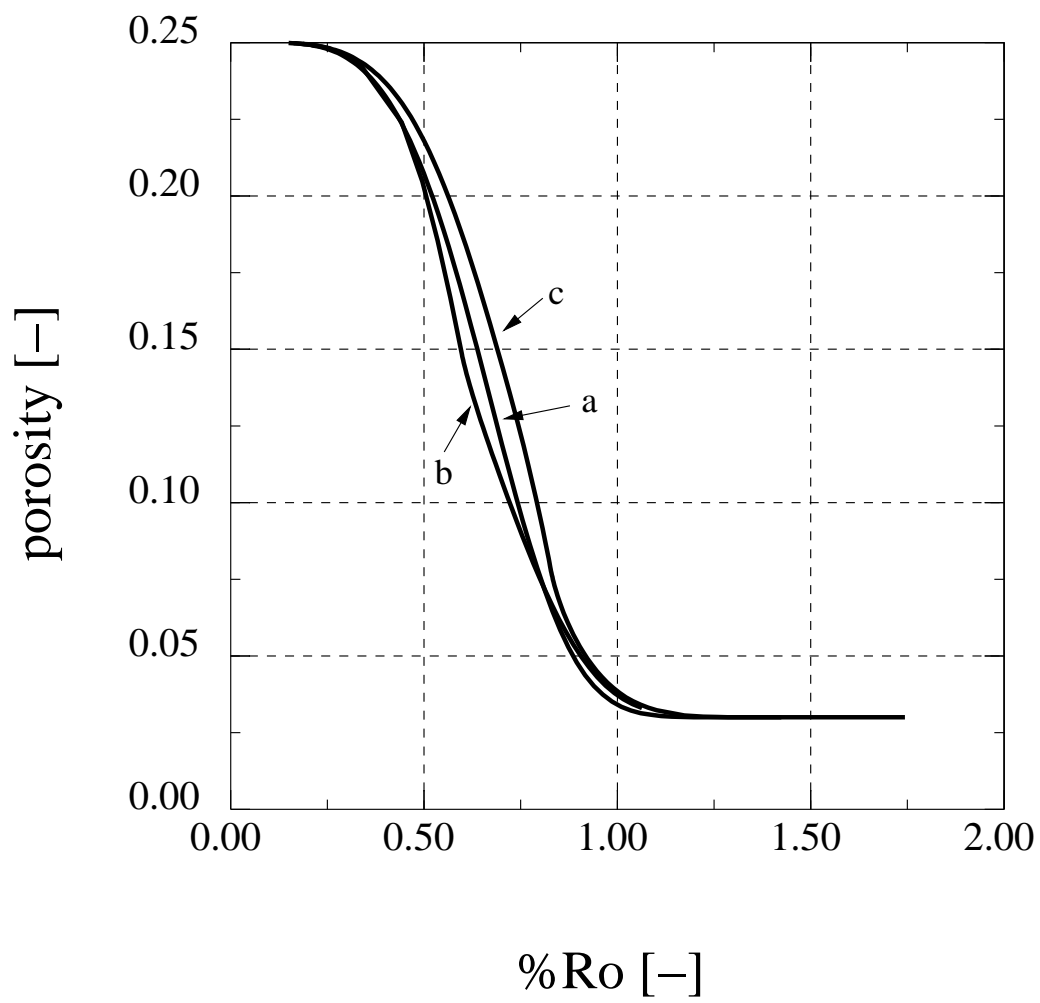
file: fig2c.eps



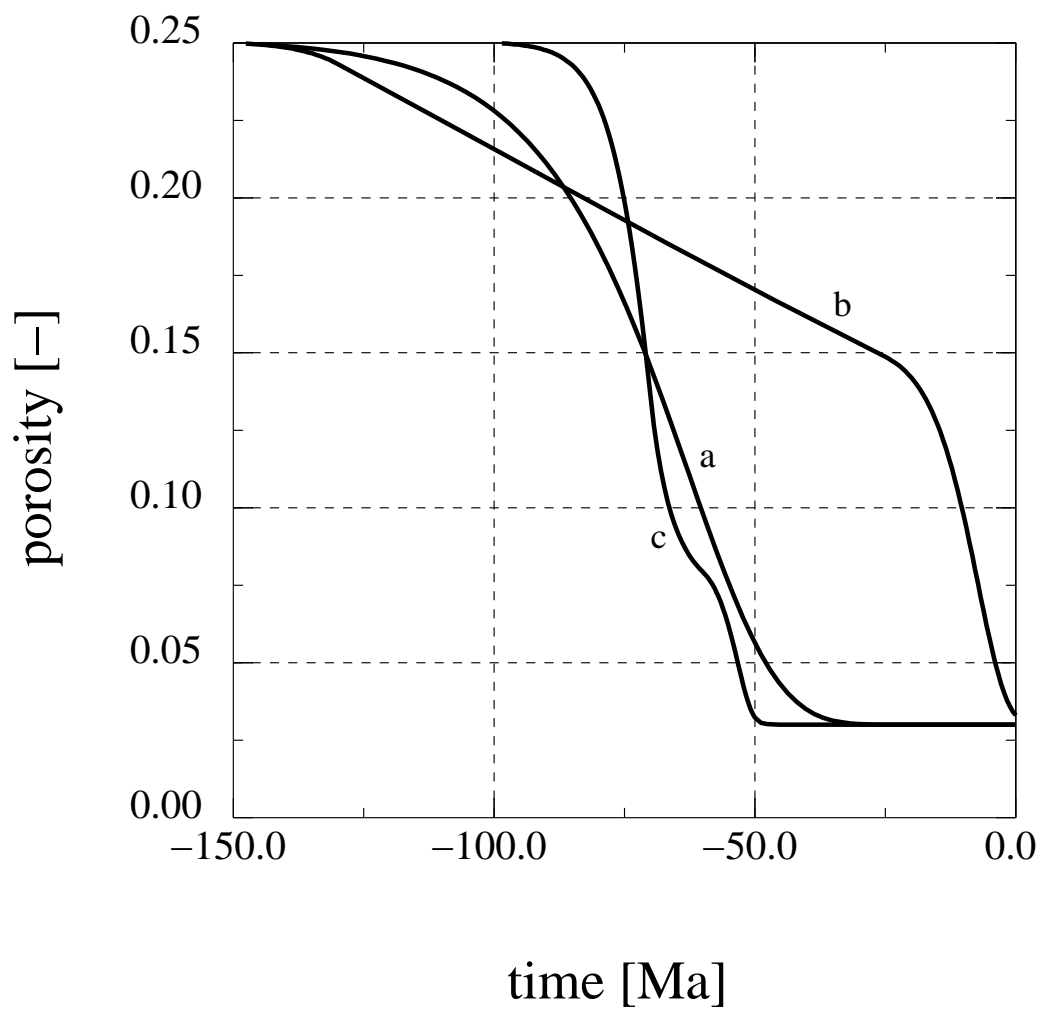
file: fig3a.eps



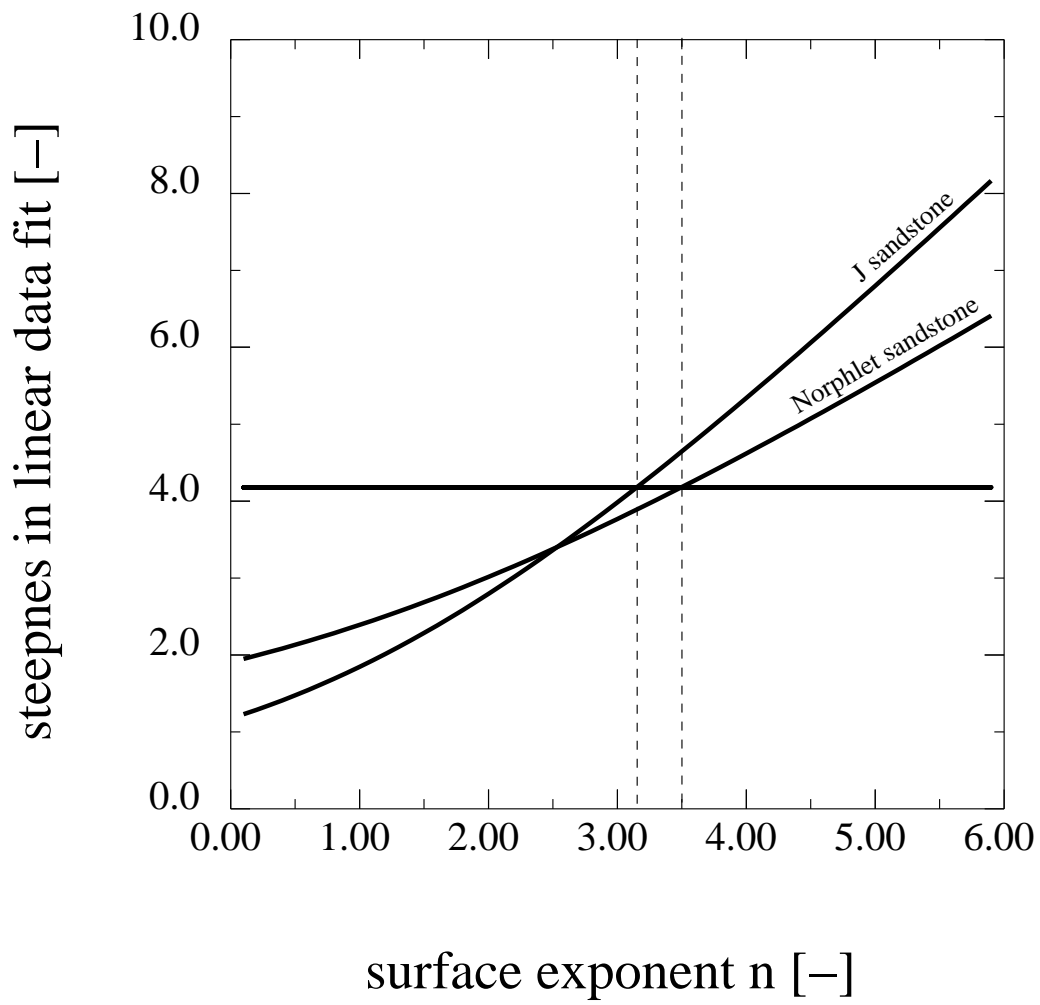
file: fig3b.eps



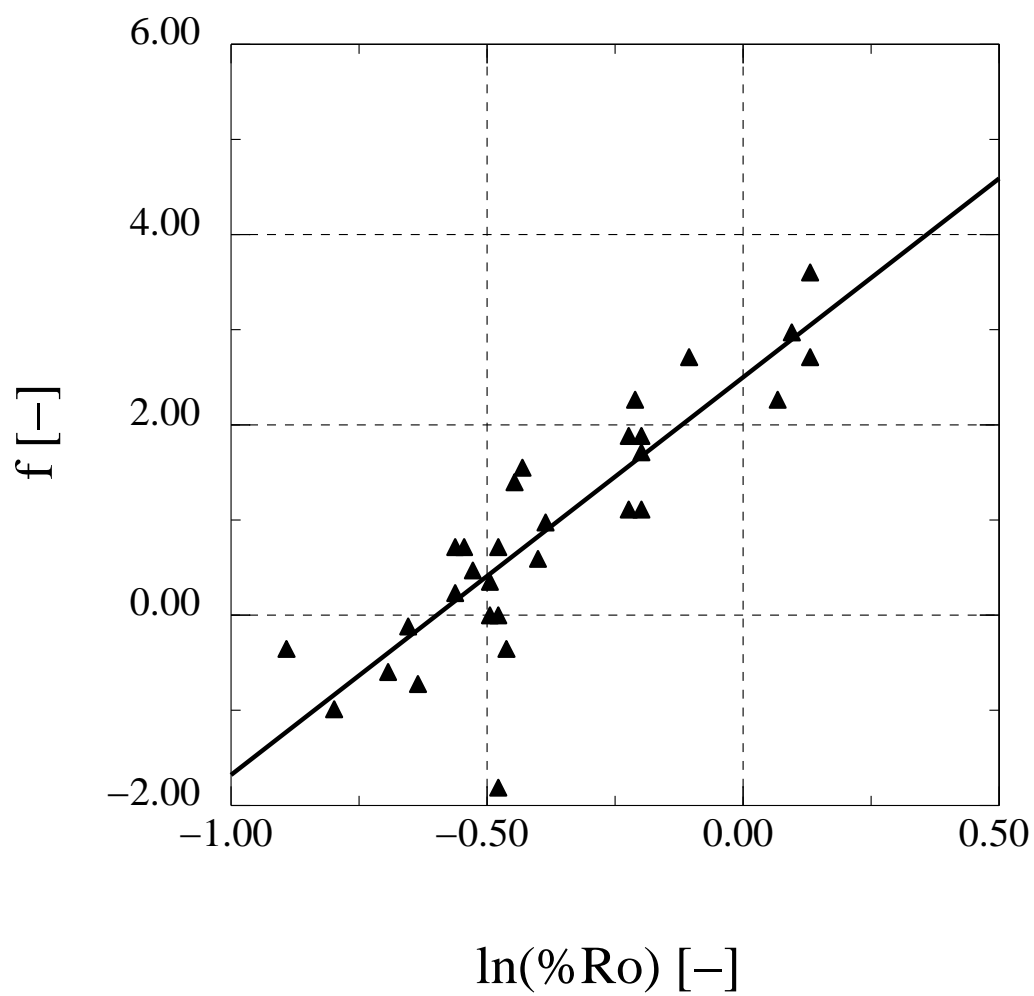
file: fig3c.eps



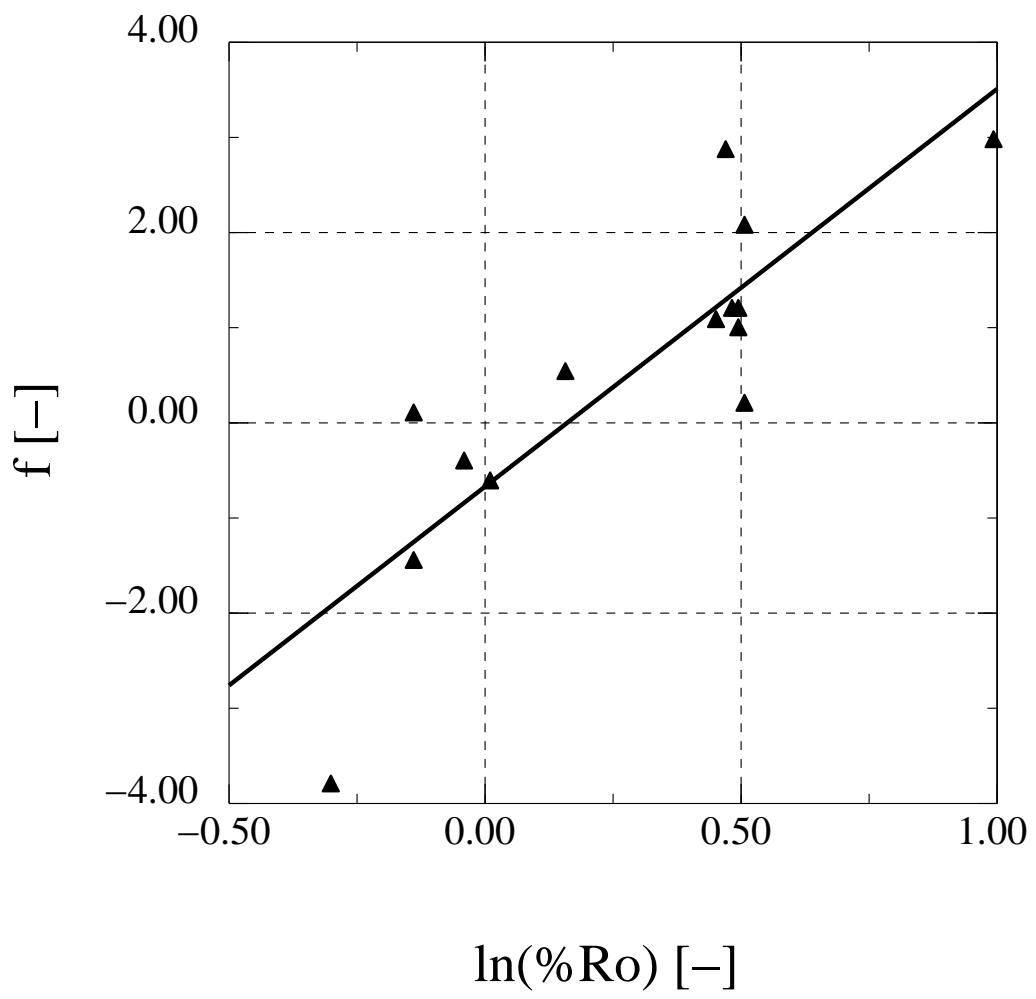
file: fig3d.eps



file: fig4.eps



file: fig5.eps



file: fig6.eps

13 Tables

Symbol	Value	Units
v_q	$2.4 \cdot 10^{-5}$	$\text{m}^3 \text{mole}^{-1}$
a_I	0.069	$^{\circ}\text{C}^{-1}$
b_I	$2.19 \cdot 10^{-17}$	s^{-1}
a_ϕ	0.051	$^{\circ}\text{C}^{-1}$
b_ϕ	$1.98 \cdot 10^{-18}$	$\text{mole m}^{-2} \text{s}^{-1}$
p	0.175	-
q	-0.732	-
ϕ_c	0.26	-
ϕ_0	0.03	-
S_0	$5 \cdot 10^4$	m^2/m^3
n	1	-

Table 1: The rate of quartz cementation is given by Walderhaug (1994a) as $r(T) = 1.98 \cdot 10^{-22} \cdot 10^{0.022T}$ in units $\text{mole cm}^{-2} \text{s}^{-1}$, which becomes $r(T) = b_\phi e^{a_\phi T}$ in units $\text{mole m}^{-2} \text{s}^{-1}$. The TTI-integral is $\text{TTI} = \int_{t_0}^{t_1} 2^{-10.5} \cdot 2^{0.1T} dt$ with t in unit Ma (McKenzie 1981), and it becomes $\text{TTI} = \int_{t_0}^{t_1} b_I e^{a_I T} dt$ when t is in unit s.

14 Captions

Figure 1: The dimensionless specific surface $\hat{S}(\phi)$ is plotted as a function of the porosity for different exponents n .

Figure 2a: The porosity reduction from quartz cementation is plotted as a function of temperature for different heating rates. Heating is from 0 °C to 180 °C for the time intervals a=260 Ma, b=130 Ma, c=65 Ma and d=32.5 Ma.

Figure 2b: The porosity as a function of temperature in figure 2a is plotted as a function of %Ro.

Figure 2c: The porosity represented by f_1 -values (the inverse specific surface integrated over porosity) is plotted as $\ln(\%Ro)$ for the same heating rates as in figure 1a.

Figure 3a: The porosity represented by f_1 -values (the inverse specific surface integrated over porosity) is plotted as $\ln(\%Ro)$ for the three different temperature histories shown in figure 3b.

Figure 3b: Three different temperature histories.

Figure 3c: The porosity as a function of %Ro for the three different temperature histories in figure 3b.

Figure 3d: The porosity as a function of time for the three different temperature histories in figure 3b.

Figure 4: The steepness of a linear least square minimization is plotted for the J sandstone and the Norphlet sandstone as a function of the exponents in the specific surface function from 0 to 6. The horizontal line is the steepness required by the line (13).

Figure 5: The optimal match of the line (13) against the data set for the J sandstone, where data is taken from Schmoker and Higley (1991).

Figure 6: The optimal match of the line (13) against the data set for the Norphlet sandstone, where the data is taken from Schmoker and Schenk (1994).